

**The kinetic isotope effect in the reaction of O(3 P) with H<sub>2</sub>, D<sub>2</sub>, and HD**

Nathan Presser and Robert J. Gordon

Citation: *The Journal of Chemical Physics* **82**, 1291 (1985); doi: 10.1063/1.448451View online: <http://dx.doi.org/10.1063/1.448451>View Table of Contents: <http://scitation.aip.org/content/aip/journal/jcp/82/3?ver=pdfcov>Published by the **AIP Publishing**

---

**Articles you may be interested in**[The intramolecular kinetic isotope effect for the reaction O\(3 P\)+HD](#)J. Chem. Phys. **92**, 7382 (1990); 10.1063/1.458224[Energy dependence, kinetic isotope effects, and thermochemistry of the nearly thermoneutral reactions N+\(3 P\)+H<sub>2</sub>\(HD,D<sub>2</sub>\)→NH+\(ND<sup>+</sup>\)+H\(D\)](#)J. Chem. Phys. **86**, 2659 (1987); 10.1063/1.452068[Reaction dynamics for O\(3 P\)+H<sub>2</sub>, D<sub>2</sub>, and HD. VI. Comparison of TST and reduced dimensionality quantum and quasiclassical isotope effects with experiment](#)J. Chem. Phys. **86**, 1976 (1987); 10.1063/1.452148[Calculation of H/D Kinetic Isotope Effects for the Reactions of Trifluoromethyl Radicals with SiH<sub>4</sub>](#)J. Chem. Phys. **54**, 1919 (1971); 10.1063/1.1675119[Photolysis of Hexafluoroacetone in the Presence of H<sub>2</sub>, D<sub>2</sub>, and HD. Kinetic Isotope Effects in the Reaction of CF<sub>3</sub> with Molecular Hydrogen](#)J. Chem. Phys. **49**, 4825 (1968); 10.1063/1.1669966

---



# The kinetic isotope effect in the reaction of $O(^3P)$ with $H_2$ , $D_2$ , and $HD$

Nathan Presser and Robert J. Gordon

Department of Chemistry, University of Illinois at Chicago, Chicago, Illinois 60680

(Received 17 July 1984; accepted 14 August 1984)

The reaction of  $O(^3P) + H_2$ ,  $D_2$ , and  $HD$  was studied by the flash photolysis-resonance fluorescence method. The rate constants  $k_{XY}(T)$  were measured over the temperature ranges 297–471 K for  $XY = H_2$ , 422–472 K for  $D_2$ , and 422–473 K for  $HD$ . Above 400 K  $k_{H_2}$  are in excellent agreement with earlier flow measurements, but below this temperature most of the flow data are systematically lower. A small deviation from the Arrhenius function was observed for  $k_{H_2}$  at 297 K. Our measurements of  $k_{D_2}$  are in excellent agreement with the results of Westenberg and deHaas and differ from those Clyne and Thrush. The measured values of  $k_{HD}$  equal the arithmetic mean of  $k_{H_2}$  and  $k_{D_2}$  within experimental error. A detailed comparison is made between the present results and the CEQB calculations of Bowman, Wagner, Walch, and Dunning and the ICVT/LAG calculations of Garrett and Truhlar. Good overall agreement is obtained with both theories.

## I. INTRODUCTION

The reaction of oxygen atoms with hydrogen molecules has been a benchmark system in experimental and theoretical kinetics. The experimental work through 1982 has been reviewed by Cohen and Westberg.<sup>1</sup> The thermal rate constant  $k_{H_2}$  for the reaction



has been measured by various flow methods over the temperature range 298–1067 K and in shock tubes between 1200 and 2800 K. Over the entire experimental temperature range the measured rate constants span six orders of magnitude, with a typical uncertainty of  $\pm 25\%$  at any given temperature. In addition, a single measurement for  $O(^3P) + H_2$  ( $v = 1$ ) has been performed at room temperature.<sup>2</sup>

For the isotopic reaction



only three studies have been reported to date. Westenberg and deHaas<sup>3</sup> and Clyne and Thrush<sup>4</sup> measured  $k_{D_2}$  in flow reactors over the temperatures ranges 416–968 and 491–671 K, respectively, while Pamidimukkala and Skinner<sup>5</sup> covered the range 2097–2481 in a shock tube. There is a strong discrepancy between the first two studies, with the ratio  $k_{H_2}/k_{D_2}$  differing by a factor of 2. The rate constant  $k_{HD}$  for  $O + HD$  has not been previously reported.<sup>6</sup>

This reaction has also been the subject of numerous theoretical studies. Most of the work prior to 1982 has been summarized by Schatz.<sup>7</sup> Recently Bowman, Dunning, Schatz, Wagner, and their co-workers<sup>8–13</sup> initiated an extensive study of this system with the goal of obtaining a chemically accurate potential energy surface and of developing reliable and inexpensive dynamical techniques which could be tested on that surface. In a series of papers they compared the experimental rate constants with collinear quasiclassical

trajectories, exact collinear quantum mechanical scattering calculations, and canonical transition state theory, utilizing several potential energy surfaces. Of the five surfaces tested, a modified form of the *ab initio* POLCI surface of Lee *et al.*<sup>9</sup> and the *ab initio* surface of Schinke and Lester<sup>14</sup> displayed the best overall agreement with experiment.

One theoretical approach developed by these workers which proved to be particularly useful is a reduced dimensionality calculation<sup>12</sup> in which the exact collinear quantum (CEQ) mechanical transmission coefficient is used to correct the canonical transition state theory rate constant. In their most recent version, denoted the CEQB method,<sup>11</sup> the bending eigenvalue was added adiabatically to the collinear modified POLCI surface of Lee *et al.*<sup>9</sup> The resulting quantum mechanical transmission coefficient was again used to correct the transition state theory rate constant. Both the CEQ and CEQB rate constants are in excellent agreement with the thermal measurements, but only the CEQB calculation agrees with the  $O + H_2$  ( $v = 1$ ) point.<sup>2</sup> The CEQB method was also used to calculate the isotope effect. Their calculated ratio  $k_{H_2}/k_{D_2}$  is in good agreement with the results of Westenberg and deHaas<sup>3</sup> and of Pamidukkala and Skinner,<sup>5</sup> and disagrees with those of Clyne and Thrush.<sup>4</sup>

In another study, Truhlar and co-workers<sup>15,16</sup> used variational transition state theory with various semiclassical approximations to the tunneling coefficient to calculate the thermal rate constant. These calculations are in good qualitative agreement with the results of Bowman *et al.*<sup>11</sup>

In a third theoretical study, Broida and Persky<sup>17</sup> performed 3D quasiclassical trajectory calculations using various model LEPS surfaces. Although this study necessarily ignored tunneling effects, which are very large near room temperature, they were able to obtain good agreement with experiment for the Johnson and Winter<sup>18</sup> surface.

The objective of the present work is to obtain reliable values for  $k_{H_2}$ ,  $k_{D_2}$ , and  $k_{HD}$  which could be used to test the theoretical calculations. All previous determinations of these rate constants below shock tube temperatures were performed in flow reactors with high concentrations of oxygen atoms. In many of these studies complicated stoichiometric

tric corrections were invoked to extract the rate constant. Our previous experience with similar atom-diatom reactions<sup>19-22</sup> has demonstrated the importance of performing real-time measurements with very low atom concentrations to guard against possible secondary reactions and heterogeneous effects. The existence of rapid secondary sinks for oxygen atoms and the substantial scatter in rate constants reported from the same laboratory<sup>23-25</sup> further emphasize the need for an independent real-time study of this system.

## II. EXPERIMENTAL METHODS

The method used in this study was flash photolysis with resonance fluorescence detection (FP-RF) of oxygen atoms. A detailed description of the apparatus and experimental procedure has been presented previously.<sup>21</sup> The only modification to the apparatus was the introduction of an 18 mm i.d. Pyrex tube between the resonance lamp and the reaction chamber. This tube acted as a light pipe, increasing the flux of resonance radiation in the viewing region by a factor of 3 to 4 and obviating the need for all but one of the resonance lamp collimators.

In the FP-RF method a precursor molecule is photolyzed to produce the atomic or radical reactant [in this case  $O(^3P)$ ], while the concentration of reactants and/or products are monitored spectroscopically in real time. This technique greatly reduces wall effects and, because of the sensitivity of RF detection, allows very low concentrations of reactants to be used. It has the drawback, however, that the precursor must satisfy several stringent requirements, some of which may be difficult to fulfill simultaneously. Specifically, the precursor must have a large UV absorption cross section at wavelengths longer than the LiF cutoff; it must have a small absorption cross section at the RF wavelength; it must be thermally stable at the temperatures of interest; and it must not react rapidly with the atomic or radical fragment at these temperatures. The only molecule we could find that satisfies all of these properties for the generation and detection of  $O(^3P)$  is  $O_2$ .

The presence of molecular oxygen in the gas mixture can lead to complicated side reactions, and great care must be taken to avoid such effects. One of these is the formation of the highly reactive  $HO_2$  radical. As is shown in the following section, this problem can be eliminated by working with very low  $O_2$  concentrations. A second potential complication is the production of  $O(^1D)$ , which reacts with  $H_2$  much faster than does  $O(^3P)$ . Although  $O(^1D)$  formation was suppressed in some runs by filtering the flash lamp with quartz windows and with 20 Torr of  $O_2$  in the flash lamp collimating region, this precaution turned out not to be necessary so long as only the  $O(^3P)$  fluorescence was detected. To do this, it is necessary to block the very strong hydrogen RF Lyman- $\alpha$  signal which results from the  $O(^1D) + H_2$  reaction. This was accomplished by placing a 2 mm thick  $CaF_2$  filter in front of the photomultiplier tube. In addition, in order to reduce the scattered background signal produced by nonresonant radiation from the resonance lamp, a 6 Torr  $O_2$  filter was placed between the resonance lamp and the reactor cell.

In the FP-RF technique, the decay rate of the detected species is the sum of two terms, one due to chemical reaction and the other due to diffusion out of the field of view. The second term is usually much smaller than the first and can be measured independently by monitoring the decay rate in a nonreactive mixture (i.e., one in which hydrogen is absent). This procedure also corrects for reactions with any impurities that might be present in the inert carrier gas (in this case argon) or in the precursor gas. In the nonreactive mixtures used to measure the diffusive rate, hydrogen was replaced by an equal partial pressure of He. The assumption made in this procedure is that hydrogen contributes very little to the total diffusive rate, and that this contribution can be approximated by substituting an inert gas of comparable mass. While this method is satisfactory for small mole fractions of hydrogen, care must be taken for hydrogen-rich mixtures. At the lowest temperatures studied, mixtures as rich as 72%  $H_2$  and 28% Ar were used. In this extreme case substitution of  $H_2$  by He could possibly lead to significant errors in the diffusive correction. However, we demonstrated in a series of test runs with different mole fractions of He and Ar that the diffusive rate is determined almost exclusively by the partial pressure of Ar. Hence we concluded that replacement of  $H_2$  by He in the diffusion measurements contributed negligibly to the error in the diffusive correction. This correction was usually less than 5%, and never greater than 15%, of the total decay rate in those experimental runs which were used for extracting rate constants.

Gas mixtures were prepared in advance and stored in 50 l Pyrex bulbs. Reactive mixtures consisted of Ar carrier gas containing the hydrogen isotope of interest and 15 to 480 ppm  $O_2$ . The hydrogen concentrations used were 4.9% to 72%  $H_2$ , 2.5% to 63%  $D_2$ , and 4.9% to 20% HD. The total gas pressure ranged from 100 to 600 Torr. The gases used were Matheson grade  $H_2$  (< 5 ppm total impurities), Matheson  $O_2$  zero gas (< 0.5 ppm hydrocarbons), and Matheson grade Ar (< 5 ppm total impurities). The manufacturer's stated impurities in  $D_2$  (Matheson C. P. grade) are 0.1% HD and < 1 ppm total hydrocarbons. The  $H_2$  and  $D_2$  gases were further purified by slowly flowing them through a room temperature molecular sieve followed by a liquid  $N_2$  trap. The molecular sieve had been previously degassed at 200 °C for 24 h. HD was synthesized by reaction of  $LiAlH_4$  with  $D_2O$ .<sup>26</sup> Mass spectrometric analysis indicated that the isotopic impurities in HD were  $2.5 \pm 2.0\%$   $H_2$  and < 0.5%  $D_2$ . All rate constants quoted in this paper are corrected for uncertainties in the isotopic purity of the reactants.

## III. KINETIC ANALYSIS

The experiments were always carried out under pseudo-first-order conditions, with  $[O] \ll [H_2]$ ,  $[D_2]$ , or  $[HD]$ . [Unless indicated otherwise, O always refers to  $O(^3P)$ .] Under these conditions, one might expect the O decay after correction for diffusion to equal  $k_{XY}[XY]$ , where X and Y are H or D. However, because of complicating secondary reactions, this is not always the case.

There are two principle O atom sinks which must be considered. One is the reaction



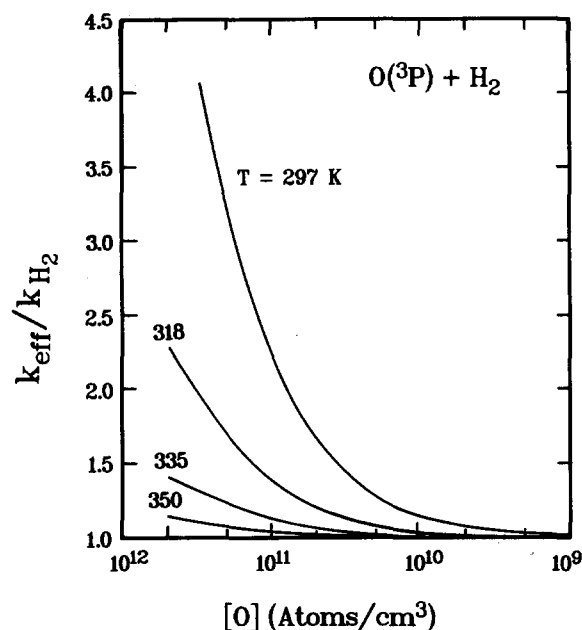
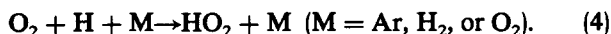


FIG. 1. Predicted ratio of the effective rate constant  $k_{\text{eff}}$  to the known value of  $k_{\text{H}_2}$ , as a function of the initial concentration of oxygen atoms. Details of the calculation are provided in the text.

and its deuterium analog. This reaction occurs regardless of the choice of oxygen atom precursor. The second sink is a consequence of using  $\text{O}_2$  for generating O atoms. In this case the  $\text{HO}_2$  (or  $\text{DO}_2$ ) radical is formed in the three body reaction (illustrated for  $\text{X} = \text{H}$ ),



$\text{HO}_2$  can then react rapidly with O, H, and  $\text{HO}_2$ , as follows:

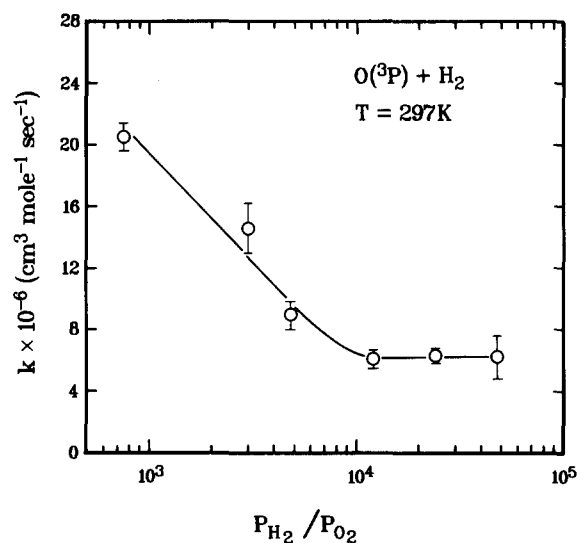


FIG. 2. Experimental values of  $k_{\text{eff}}$  for different gas mixtures. The mole fraction of  $\text{H}_2$  varied from 18% to 72% while the mole fraction of  $\text{O}_2$  was 0.047% to 0.0015%.

TABLE I. Measured rate constants for the reaction of  $\text{O}(^3\text{P})$  with hydrogen molecules.

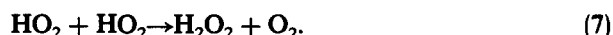
Isotope	$T^a$ (K)	Gas composition (%)	$k \times 10^{-8}$ ( $\text{cm}^3 \text{mol}^{-1} \text{s}^{-1}$ )
$\text{H}_2$	296.6	71.8, 0.006 <sup>b</sup>	$0.0618 \pm 0.0057^c$
	318.0	71.8, 0.006	$0.116 \pm 0.011$
	335.0	71.8, 0.012	$0.221 \pm 0.017$
	350.2	71.8, 0.012	$0.350 \pm 0.034$
	370.2	71.8, 0.04	$0.645 \pm 0.019$
	395.7	18.2, 0.047	$1.32 \pm 0.07$
	422.3	18.3, 0.047	$2.33 \pm 0.22$
	446.8	5.0, 0.047	$4.58 \pm 0.23$
	471.1	5.0, 0.047	$6.99 \pm 0.39$
$\text{D}_2$	422.4	35.7, 0.048	$0.379 \pm 0.046$
	445.7	35.7, 0.048	$0.817 \pm 0.051$
	472.5	9.5, 0.046	$1.62 \pm 0.13$
$\text{HD}$	422.3	10.0, 0.047	$1.50 \pm 0.11$
	446.7	9.0, 0.045	$2.67 \pm 0.17$
	471.7	9.0, 0.045	$4.48 \pm 0.32$

<sup>a</sup> Temperatures are accurate to  $\pm 0.5$  K.

<sup>b</sup> The two entries are, respectively, the mole fractions of hydrogen isotope and of  $\text{O}_2$  at the onset of convergence.

<sup>c</sup> Uncertainties are one standard deviation.

and



The important OH radical is scavenged by



and to a minor extent by



A more comprehensive model, including the chemistry of  $\text{H}_2\text{O}_2$  and  $\text{O}_3$ , is employed in the sensitivity analysis of Dougherty and Rabitz.<sup>27</sup>

To deal with these complications several of the previous investigators introduced a steady state correction factor which enabled them to extract  $k_{\text{XY}}$  from the observed reac-

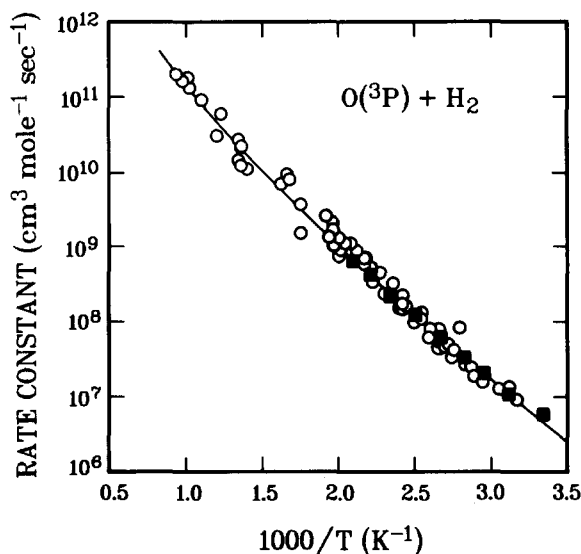


FIG. 3. Comparison of the present values of  $k_{\text{H}_2}$  (solid symbols) with the previous flow measurements. The curve is the recommended fit of Cohen and Westberg (Ref. 1).

tion rate. An advantage of our real-time measurements is that it is possible to find experimental conditions under which these secondary reactions contribute very little to the observed decay rate of O, so that stoichiometric corrections are unnecessary. To find suitable experimental conditions we integrated the rate equations for reactions (1) and (3)–(9) and calculated the time dependent concentrations of O, H, OH, and HO<sub>2</sub>. The effective rate constant  $k_{\text{eff}}$  was then obtained from the logarithmic slope of  $[O(t)]$ . The results of a typical calculation are shown in Fig. 1. The conditions in this calculation were a total pressure of 200 Torr, with 72% H<sub>2</sub>, 0.01% O<sub>2</sub>, and variable initial concentrations of O. To account for the possible effect of O(<sup>1</sup>D), it was further assumed that equal amounts of O(<sup>3</sup>P) and O(<sup>1</sup>D) are produced by the flash, but that O(<sup>1</sup>D) reacts with H<sub>2</sub> instantaneously to form H + OH at  $t = 0$ . Ignoring this effect and setting  $[H(t = 0)] = [OH(t = 0)] = 0$  did not affect the conclusions of this study. As illustrated in Fig. 1, the ratio  $k_{\text{eff}}/k_{\text{H}_2}$  approaches unity as  $[O(t = 0)]$  is reduced and as the temperature  $T$  is raised. Since a lower limit to the concentration of O(<sup>3</sup>P) that we could detect is 10<sup>9</sup> atoms/cm<sup>3</sup>,  $k_{\text{H}_2}(T)$  could not be determined by this convergence procedure below room temperature.

The general conclusions of this simulation, resulting from a wide variety of initial conditions, are as follows: (i) The effective rate constant obtained by ignoring the secondary reactions is always an upper bound to the true value. (ii) The ratio  $k_{\text{eff}}/k_{\text{H}_2}$  can be reduced by either decreasing  $[O(t = 0)]$  or by increasing  $[H_2]$ . (iii) Results (i) and (ii) are unaltered by the presence of O(<sup>1</sup>D). Further calculations including the formation of O<sub>3</sub> showed that this species also had no effect on  $k_{\text{eff}}$ .

Since  $[O(t = 0)]$  is approximately proportional to  $[O_2]$ , the conclusion of this study is that  $k_{\text{eff}}/k_{\text{H}_2}$  approaches unity monotonically as  $[H_2]/[O_2]$  is increased. This prediction

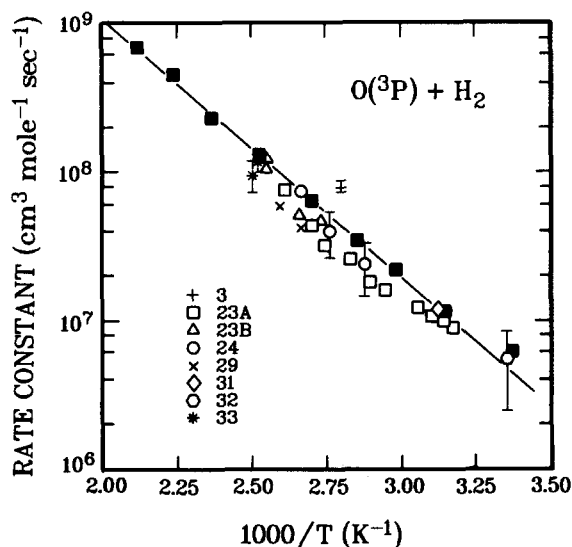


FIG. 4. Expanded display of Fig. 3 comparing the present data (solid symbols) with the low temperature flow measurements. References for the flow data are listed on the left. Error bars for Refs. 23 and 29 are unavailable. The line is a least square fit of  $\log k_{\text{H}_2}$  vs  $1/T$ , excluding the lowest temperature point.

was tested experimentally by measuring  $k_{\text{eff}}$  as a function of the gas composition ratio  $[H_2]/[O_2]$ . First we increased the mole fraction of H<sub>2</sub> by factors of  $\sim 2$  up to a maximum of 72%. The O<sub>2</sub> mole fraction was then reduced by factors of  $\sim 2$  down to a minimum of 0.0015%. The results for  $T = 296.6$  K are shown in Fig. 2. Each point represents the average of 8 to 20 runs performed at 2 to 5 different total gas pressures. The “converged” value of  $k_{\text{eff}}$  at large values of  $[H_2]/[O_2]$  is taken to be the true value of  $k_{\text{H}_2}$ . Generally, for each of the hydrogen isotopes, when the value of  $k_{\text{eff}}$  did not drop by more than 5% from the result obtained with the previous mixture,  $k_{\text{eff}}$  was taken to be converged.

#### IV. RESULTS

The experimental rate constants determined by the convergence procedure described in the previous section are summarized in Table I. The gas compositions listed in the table refer to the concentrations at which  $k_{\text{eff}}$  first converged. Generally one or two further dilutions of O<sub>2</sub> were used beyond this point. The values of  $k_{\text{XY}}$  listed in the table were obtained by a weighted nonlinear least squares fit of the exponentially decaying signal using Poisson weighting factors.<sup>28</sup> The quoted uncertainty in  $k_{\text{XY}}$  at each temperature is a single weighted standard deviation for all the converged measurements.

The rate constants in Table I are shown by the solid symbols in Figs. 3–7. In Fig. 3  $k_{\text{H}_2}$  is compared with all previously reported measurements below shock tube tem-

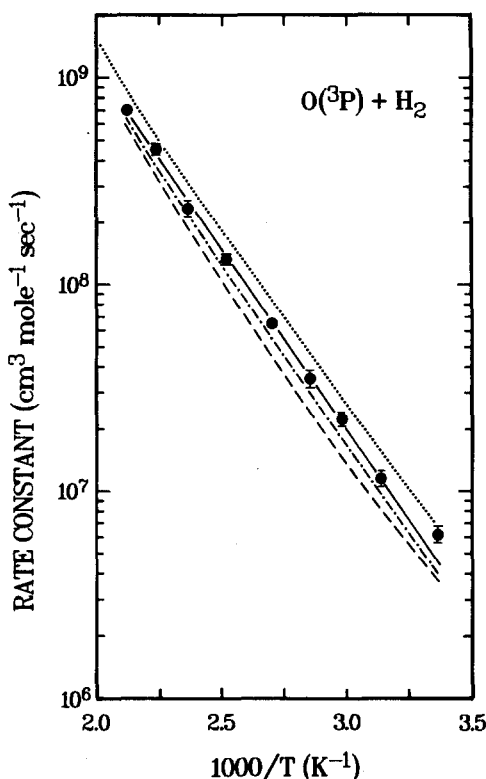


FIG. 5. Comparison of experimental and theoretical values of  $k_{\text{H}_2}$ . The points are the present results, while the solid line is a least squares fit excluding the lowest point. The dot-dashed curve is the recommendation of Cohen and Westberg (Ref. 1). The dotted curve is the CEQB calculation of Bowman *et al.* (Refs. 11 and 35) while the dashed curve is the ICVT/LAG calculation of Truhlar *et al.* (Ref. 16).

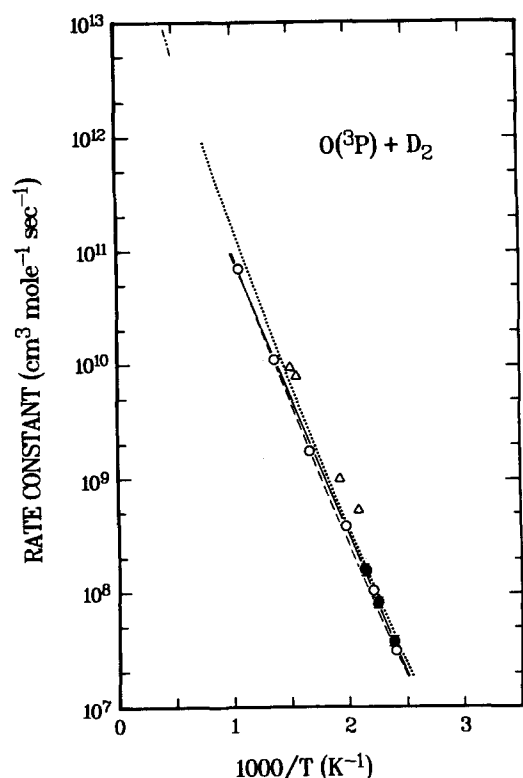


FIG. 6. Comparison of experimental and theoretical values of  $k_{D_2}$ . The solid circles are the present results, the open circles are those of Westenberg and deHaas (Ref. 3), the triangles are those of Clyne and Thrush (Ref. 4), and the very high temperature results are the shock tube data of Pamidukkala and Skinner (Ref. 5). The solid line is an Arrhenius fit to our data and those of Westenberg and deHaas. The dotted and dashed curves are, respectively, the CEQB and ICVT/LAG calculations.

peratures.<sup>3,4,23-25,29-33</sup> The excellent agreement above 400 K shows that systematic errors in the flow measurements were not a serious problem. The low temperature region ( $T < 400$  K) is plotted in more detail in Fig. 4. Here we see that most of the flow measurements were systematically lower than the present results. Since the rate constant at these temperatures is dominated by tunneling,<sup>10,11,15</sup> any deviation from a linear Arrhenius plot is especially interesting. The strong curvature seen in the measurements of Campbell and Handy<sup>23</sup> is absent in our data. However, we do find at 296.6 K that  $k_{H_2}$  lies  $37 \pm 13\%$  above the Arrhenius extrapolation. This result is statistically significant at the 99% confidence level.<sup>34</sup> It is unlikely that this deviation is caused by impurities in  $H_2$ . Such a large discrepancy would require 5 ppm of  $C_2H_4$ , for example, which is an order of magnitude greater than the upper limit set by mass spectrometric and gc analysis of our  $H_2$  gas.<sup>22</sup> A hot atom effect such as that proposed for  $Cl + D_2$ <sup>22</sup> also appears unlikely, both because  $[O(t)]$  never showed any evidence of nonexponential decay and also because  $k_{eff}$  is independent of  $[O_2]$  at the three highest dilutions in Fig. 2.

Our measured values of  $k_{D_2}$  are compared with the flow tube results in Fig. 6. Our values are found to be in excellent agreement with those of Westenberg and deHaas,<sup>3</sup> while both the slope and magnitude of the data of Clyne and Thrush<sup>4</sup> differ markedly.

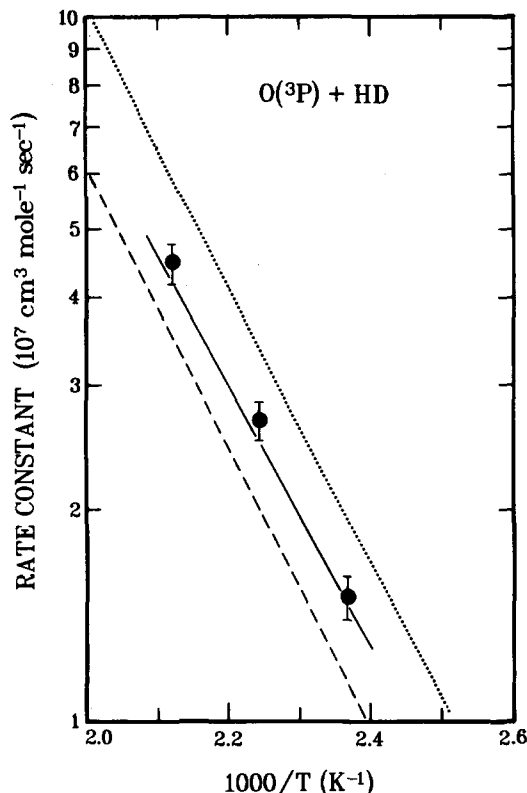


FIG. 7. Comparison of experimental and theoretical values of  $k_{HD}$ . The points are the present results. The solid curve is our experimental value of  $(k_{H_2} + k_{D_2})/2$ , while the dotted and dashed curves are the CEQB and ICVT/LAG calculations, respectively. In all cases  $k_{HD}$  refers to the sum of both product channels.

Our results for  $k_{HD}$  are shown in Fig. 7. It is curious that, within experimental error,  $k_{HD}$  is approximately equal to the arithmetic mean of  $k_{H_2}$  and  $k_{D_2}$ , which is shown by the solid curve.

## V. DISCUSSION

In Figs. 5–8 we compare our experimental results with the theoretical calculations of Bowman *et al.*<sup>11,35</sup> and those of Truhlar *et al.*<sup>15,16</sup> Both calculations utilized the rotated Morse-Spline (RMOS) fit of the modified POLCI surface of Lee *et al.*<sup>9</sup> In the first calculation an exact collinear (CEQB) transmission coefficient was used to incorporate tunneling effects into conventional transition state theory. An important feature of this calculation is the treatment of bent collision geometries. The electronic state of  $O(^3P) + H_2$ , which is degenerate for the collinear case, splits into the  $A'$  and  $A''$  states for bent configurations. Renner-Teller coupling<sup>36</sup> of the vibrational and electronic angular momenta of these states was used to calculate the adiabatic potential energy surfaces. In the CEQB treatment the lowest harmonic bending frequency of the lowest Renner-Teller vibronic state was used to calculate the transmission coefficient. This frequency is approximately equal to the arithmetic mean of the  $A'$  and  $A''$  bending frequencies.

The calculation of Truhlar *et al.*<sup>15,16</sup> utilizes the improved canonical variational transition state (ICVT) theory.<sup>37,38</sup> Tunneling is introduced by using an appropriate



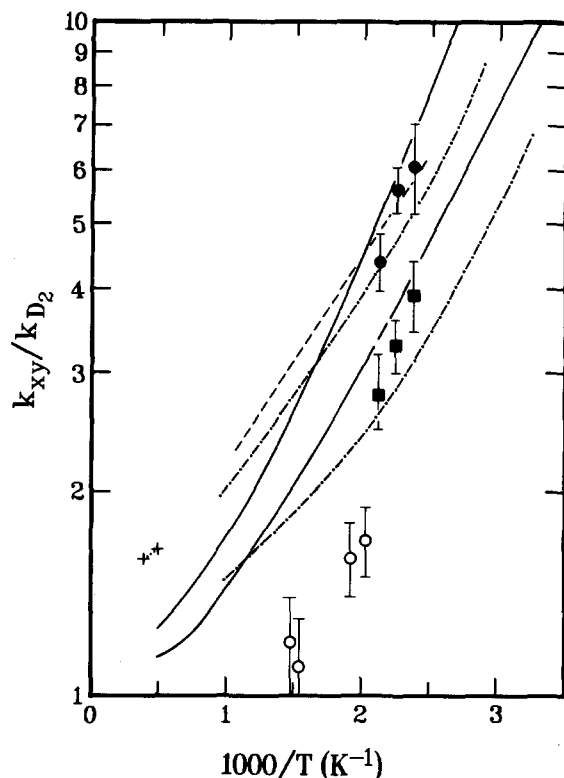


FIG. 8. Comparison of experimental and theoretical values of the isotope effect ratio  $k_{XY}/k_{D_2}$ . The solid circles and squares are the present results for  $H_2$  and  $HD$ , respectively. The dashed curve, the open circles and the crosses are from Refs. 3, 4, and 5, respectively. The solid curves are the CEQB calculations and the dot-dashed curves are the ICVT/LAG calculations. In each calculation the upper curve is the  $H_2$  result.

least-action variational ("LAG") principle to optimize a series of tunneling paths on the ground (i.e.,  $A''$ ) electronic surface. A WKB approximation is used for the stretching vibrations,<sup>39</sup> while the bending motion is described by an anti-Morse potential<sup>40</sup> with a Sato parameter adjusted to reproduce the *ab initio* harmonic bending frequency of the  $A''$  saddle point.<sup>41</sup> In addition, a quartic approximation is used for the bending anharmonicity.<sup>37</sup> The electronic partition function for the transition state includes only the  $A''$  state (i.e., it is a factor of 0.41 to 0.45 over our temperature range as compared to a factor of approximately 2/3 for the Renner-Teller treatment). The calculations of Truhlar *et al.* quoted in this paper<sup>16</sup> are identical to those of Ref. 15 except for the use of the WKB approximation for the stretching vibrations, which was not used in the earlier work.

As shown in Figs. 5–8 the experimental and theoretical results are in strikingly good agreement. The experimental rate constants lie approximately midway between the ICVT/LAG and CEQB values, with the ICVT/LAG results always below the experimental values. In Fig. 8 the isotope effect ratios,  $k_{XY}/k_{D_2}$ , are displayed. Again, the experimental points are bounded by the two theoretical predictions.

A quantitative comparison of the two calculations<sup>16,35</sup> shows that at 400 K the ratio  $k_{XY}^{CEQB}/k_{XY}^{ICVT/LAG}$  is 1.72, 1.26, and 1.73 for  $H_2$ ,  $D_2$ , and  $HD$ . This discrepancy may be due to a combination of factors, the most important being the different approximations used to calculate the transmission

coefficient and the different methods used to treat the bending motion and to account for the multiplicity of electronic surfaces.<sup>42</sup>

Another point for comparison is the departure from Arrhenius behavior. To compare theory with experiment, we fitted the theoretical calculations with an Arrhenius function at the same temperatures which were used in the experiment. The results are very similar to that shown in Fig. 4 for our data. That is, the eight highest points lie very nearly on a straight line, while the room temperature calculations lie above the line. For the CEQB calculation,  $k_{H_2}$  at 294 K lies 18.8% above the least squares Arrhenius extrapolation, while the ICVT/LAG result at 297 K is 24.6% above the line. A third point for comparison is the relation between  $k_{HD}$  and  $(k_{H_2} + k_{D_2})/2$ . For the CEQB calculation these quantities agree within 10% over our temperature range, while for the ICVT/LAG calculation they agree within 0.5%, as compared with our experimental uncertainty of ~10%. In the case of the trajectory calculation of Broida and Persky,<sup>17</sup> the arithmetic mean of  $k_{H_2}$  and  $k_{D_2}$  is 40% larger than  $k_{HD}$  for the Johnson and Winter surface.<sup>18</sup> On the whole we find that the agreement between theory and experiment is remarkably good.

## V. CONCLUSIONS

The principle findings of this study are as follows:

- (i) Real-time measurements of  $k_{H_2}$  are in good agreement with previous flow measurements above 400 K, indicating that the large scatter in the earlier work is not due to systematic errors.
- (ii) Below 400 K most of the flow measurements lie below the present results. Departure from Arrhenius behavior is observed only at room temperature.
- (iii) Our measurements of  $k_{D_2}$  are in excellent agreement with the results of Westenberg and deHaas.<sup>4</sup>
- (iv) Values for  $k_{HD}$ , which are reported for the first time, lie midway between  $k_{H_2}$  and  $k_{D_2}$ .
- (v) The measured values of  $k_{H_2}$ ,  $k_{D_2}$ , and  $k_{HD}$  are in good agreement with the CEQB reduced dimensionality calculation of Bowman *et al.*<sup>11,35</sup> and with the ICVT/LAG variational transition state theory calculation of Truhlar *et al.*<sup>15,16</sup>, both using the modified *ab initio* POLCI surface of Lee *et al.*<sup>9</sup>

## ACKNOWLEDGMENTS

The authors wish to thank Dr. Albert F. Wagner, Professor Joel M. Bowman, and Professor Donald G. Truhlar for many helpful discussions and for preprints of their forthcoming publications. We are especially grateful to them for extending their calculations to facilitate comparison of their theories with our experimental results. We also wish to thank Professor Richard Burns and Mr. Thomas Bauer for measuring the isotopic purity of our  $HD$  samples. Finally, we are very pleased to acknowledge the generous support of the Department of Energy, Office of Basic Energy Sciences, under contract no. DE-AC02-77ER04426.

<sup>1</sup>N. Cohen and K. R. Westberg, *J. Phys. Chem. Ref. Data* **12**, 531 (1983).

<sup>2</sup>G. C. Light, *J. Chem. Phys.* **68**, 2831 (1978).

<sup>3</sup>A. A. Westenberg and N. deHaas, *J. Chem. Phys.* **47**, 4241 (1967); **50**, 2512

- 2512 (1969).
- <sup>4</sup>M. A. A. Clyne and B. A. Thrush, *Proc. R. Soc. London A* **5**, 544 (1963).
- <sup>5</sup>K. M. Pamidimukkala and G. B. Skinner, *J. Chem. Phys.* **76**, 311 (1982).
- <sup>6</sup>Throughout this paper  $k_{\text{HD}}$  refers to the sum of the rate constants for producing both OH + D and OD + H. The branching ratio for these two channels is currently being measured in our laboratory.
- <sup>7</sup>G. C. Schatz, in *Potential Energy Surfaces and Dynamics Calculations for Chemical Reactions and Molecular Energy Transfer*, edited by D. G. Truhlar (Plenum, New York, 1981), p. 287.
- <sup>8</sup>G. C. Schatz, A. F. Wagner, S. P. Walch, and J. M. Bowman, *J. Chem. Phys.* **74**, 4984 (1981).
- <sup>9</sup>K. T. Lee, J. M. Bowman, A. F. Wagner, and G. C. Schatz, *J. Chem. Phys.* **76**, 3563 (1982).
- <sup>10</sup>K. T. Lee, J. M. Bowman, A. F. Wagner, and G. C. Schatz, *J. Chem. Phys.* **76**, 3583 (1982).
- <sup>11</sup>J. M. Bowman, A. F. Wagner, S. P. Walch, and T. H. Dunning, Jr., *J. Chem. Phys.* **81**, 1789 (1984).
- <sup>12</sup>A. F. Wagner, G. C. Schatz, and J. M. Bowman, *J. Chem. Phys.* **74**, 4960 (1981).
- <sup>13</sup>J. M. Bowman, G.-Z. Ju, K. T. Lee, A. F. Wagner, and G. C. Schatz, *J. Chem. Phys.* **75**, 141 (1981).
- <sup>14</sup>R. Schinke and W. A. Lester, Jr., *J. Chem. Phys.* **70**, 4893 (1979).
- <sup>15</sup>D. G. Truhlar, K. Runge, and B. C. Garrett, 20th Symp. (Int.) Combust. (in press).
- <sup>16</sup>B. C. Garrett and D. G. Truhlar (unpublished results).
- <sup>17</sup>M. Broida and A. Persky, *J. Chem. Phys.* **80**, 3687 (1984).
- <sup>18</sup>B. R. Johnson and N. W. Winter, *J. Chem. Phys.* **66**, 4116 (1977).
- <sup>19</sup>J. C. Miller and R. J. Gordon, *J. Chem. Phys.* **75**, 5305 (1981).
- <sup>20</sup>J. C. Miller and R. J. Gordon, *J. Chem. Phys.* **76**, 5167 (1982).
- <sup>21</sup>J. C. Miller and R. J. Gordon, *J. Chem. Phys.* **78**, 3713 (1983).
- <sup>22</sup>J. C. Miller and R. J. Gordon, *J. Chem. Phys.* **79**, 1252 (1983).
- <sup>23</sup>(a) I. M. Campbell and B. J. Handy, *J. Chem. Soc. Faraday Trans.* **71**, 2097; (b) **74**, 316 (1978).
- <sup>24</sup>R. N. Dubinsky and D. J. McKenney, *Can. J. Chem.* **53**, 3531 (1975).
- <sup>25</sup>V. P. Balakhnin, Yu. M. Gershenzon, V. N. Kondrat'ev, and A. B. Nalbandyan, *Dokl. Phys. Chem.* **170**, 659 (1966); V. P. Balakhin, V. I. Egorov, P. J. van Tiggelen, V. V. Azatyan, Yu. M. Gershenzon, and V. N. Kondrat'ev, *Kinet. Cataly.* **9**, 559 (1968).
- <sup>26</sup>I. Wender, R. A. Friedel, and M. Orchin, *J. Am. Chem. Soc.* **71**, 1140 (1949).
- <sup>27</sup>E. G. Dougherty and H. Rabitz, *J. Chem. Phys.* **72**, 6571 (1980).
- <sup>28</sup>P. R. Bevington, *Data Reduction and Error Analysis in the Physical Sciences* (McGraw Hill, New York 1969).
- <sup>29</sup>K. Hoyerman, H. Gg. Wagner, and J. Wolfrum, *Ber. Bunsenges. Phys. Chem.* **71**, 599 (1967).
- <sup>30</sup>V. P. Balakhnin, V. I. Egorov, and V. N. Kondrat'ev, *Dokl. Phys. Chem.* **193**, 529 (1970).
- <sup>31</sup>I. M. Campbell and B. A. Thrush, *Trans. Faraday Soc.* **64**, 1265 (1968).
- <sup>32</sup>G. C. Light and J. H. Matsumoto, *Int. J. Chem. Kinet.* **12**, 451 (1980).
- <sup>33</sup>E. L. Wong and A. E. Potter, *J. Chem. Phys.* **43**, 3371 (1965).
- <sup>34</sup>W. G. Snedecor, *Statistical Methods Applied to Experiments in Agriculture and Biology* (Iowa State College, Ames, 1956).
- <sup>35</sup>J. M. Bowman and A. F. Wagner (private communication).
- <sup>36</sup>L. B. Harding, A. G. Wagner and J. M. Bowman, *J. Chem. Phys.* (in press).
- <sup>37</sup>B. C. Garrett, D. G. Truhlar, R. S. Grev, and A. W. Magnuson, *J. Phys. Chem.* **84**, 1730 (1980); **87**, 4554 (E) (1983).
- <sup>38</sup>B. C. Garrett and D. G. Truhlar, *J. Chem. Phys.* **79**, 4931 (1983).
- <sup>39</sup>B. C. Garrett and D. G. Truhlar, *J. Chem. Phys.* **81**, 309 (1984).
- <sup>40</sup>B. C. Garrett, D. G. Truhlar, and A. W. Magnuson, *J. Chem. Phys.* **76**, 2321 (1982).
- <sup>41</sup>S. P. Walch, A. F. Wagner, T. H. Dunning, Jr., and G. C. Schatz, *J. Chem. Phys.* **72**, 2894 (1980).
- <sup>42</sup>In a further calculation, Garrett and Truhlar found that including the reaction on the A' surface increased the ICVT/LAG rate constant by ~30% for all of the isotopes.